# Assembly of Tubulin by Classic Myelin Basic Protein Isoforms and Regulation by Post-Translational Modification†

Christopher M. D. Hill, David S. Libich, and George Harauz*

*Department of Molecular and Cellular Biology and Biophysics Interdepartmental Group, University of Guelph, 50 Stone Road East, Guelph, Ontario, Canada N1G 2W1*

*Received April 7, 2005; Revised Manuscript Received October 26, 2005*

ABSTRACT: Myelin basic protein (MBP), a highly cationic protein that maintains the structure of the myelin sheath, associates with tubulin in vivo. The in vitro assembly of tubulin by MBP was examined here using several assays. The unmodified C1 component of 18.5 kDa bovine MBP (bC1) assembled tubulin into microtubules in a dose-dependent manner via filamentous intermediates, and was able simultaneously to promote the formation of microtubule bundles. The critical tubulin concentration in the presence of bC1 was 0.69 ± 0.05 $\mu$M. The effects of post-translational modifications (such as deamidation and phosphorylation) were assayed by comparing the bC1−bC6 components of 18.5 kDa bovine MBP; an increasing level of modification enhanced the ability of MBP to assemble tubulin. The effects of charge reduction via deimination were examined using recombinant murine isoforms emulating the unmodified C1 and deiminated C8 isoforms of 18.5 kDa MBP; both rmC1 and rmC8 exhibited a comparable ability to assemble tubulin. The effects of alternate exon recombination of the classic MBP variants were tested using the recombinant murine 21.5, 17.22, and 14 kDa isoforms. The isoforms containing regions derived from exon II of the classic MBP gene, 21.5 and 17.22 kDa MBP, showed no substantial difference in the extent of tubulin polymerization and bundling when compared to those of 18.5 kDa MBP. The 14 kDa isoform and two terminal deletion mutants of rmC1 were able to induce microtubule polymerization, but not bundling, to the same degree as the longer proteins. Finally, bC1 was shown to disrupt and aggregate planar sheets of crystalline tubulin stabilized by paclitaxel, establishing that these structures are not suitable substrates for the formation of MBP cocrystals.

Oligodendrocytes in the central nervous system undergo dramatic morphological changes during myelination (*1*). By remodeling their internal microfilament and microtubule networks, these cells extend membranous processes which contact and spiral around nearby neuronal axons to produce the multilamellar myelin sheath (*2*). The common microtubule-associated proteins (MAPs)[1] tau and MAP2 are expressed at low levels in oligodendrocytes (*3*−*6*), but the mechanisms that regulate the organization of microtubule networks in these cells are not yet fully understood (*7*). Myelin-associated proteins such as 2′,3′-cyclic nucleotide 3′-phosphodiesterase (CNP), myelin basic protein (MBP), and myelin-associated oligodendrocyte basic protein (MOBP) are all known to colocalize with tubulin in cultured oligodendrocytes (*5*, *7*). Tau is distributed in a pattern similar to that of MBP (*3*). In a recent detailed investigation, it has been shown that CNP interacts with tubulin in a different way than MAPs: preferential binding to tubulin heterodimers compared to microtubules and induction of microtubule assembly by copolymerization (*8*). The overexpression of CNP in both glial and nonglial cells resulted in cytoskeletal reorganization and formation of branched processes (*8*). This study is an important advance because it was not hitherto known why myelin should contain CNP, but it now appears that this protein may be involved in process outgrowth in oligodendrocytes, as an inducer (but not a stabilizer) of tubulin assembly. However, CNP is not alone in its association with tubulin in vivo.

Another major protein component in differentiated oligodendrocytes and mature myelin is the myelin basic proteins (MBPs), a family of developmentally regulated proteins that arise from different transcription start sites of the Golli (genes of the oligodendrocyte lineage) gene complex, and by

† This work was supported by a grant from the Natural Sciences and Engineering Research Council of Canada to G.H. and Ontario Graduate Scholarships held by C.M.D.H. and D.S.L.

* To whom correspondence should be addressed: Department of Molecular and Cellular Biology, University of Gueph, 50 Stone Rd. E., Guelph, ON, Canada N1G 2W1. Phone: (519) 824-4120, ext. 52535. Fax: (519) 837-2075. E-mail: gharauz@uoguelph.ca.

[1] Abbreviations: bC1−bC6, bovine MBP charge isomers (components) 1−6, respectively; bMBP, bovine MBP; CNP, 2′,3′-cyclic nucleotide 3′-phosphodiesterase; DMSO, dimethyl sulfoxide; GDP, guanosine diphosphate; GTP, guanosine 5′-triphosphate; Golli, genes of the oligodendrocyte lineage; G-PEM, GTP, PIPES, EGTA, and $MgCl_2$; MAP, microtubule-associated protein; MARCKS, myristoylated alanine-rich C-kinase substrate; MBP, myelin basic protein; MESG, 2-amino-6-mercapto-7-methylpurine riboside; MOBP, myelin-associated oligodendrocyte basic protein; MT, microtubule; $P_i$, inorganic phosphate; PNP, purine nucleoside phosphorylase; rm, recombinant murine; rmC1, recombinant murine 18.5 kDa MBP, unmodified; rmC8, recombinant murine 18.5 kDa MBP, quasi-deiminated; rmMBP, recombinant murine MBP; rmC1ΔN and rmC1ΔC, N- and C-terminal deletion mutants of rmC1, respectively; rm21, rm17, and rm14, recombinant murine 21.5, 17.22, and 14 kDa MBP, respectively; SDS−PAGE, sodium dodecyl sulfate−polyacrylamide gel electrophoresis; STOP, stable tubule only peptide; TEM, transmission electron microscope or microscopy; TMAO, trimethylamine *N*-oxide.

10.1021/bi050646+ CCC: $30.25 
Published on Web 11/23/2005

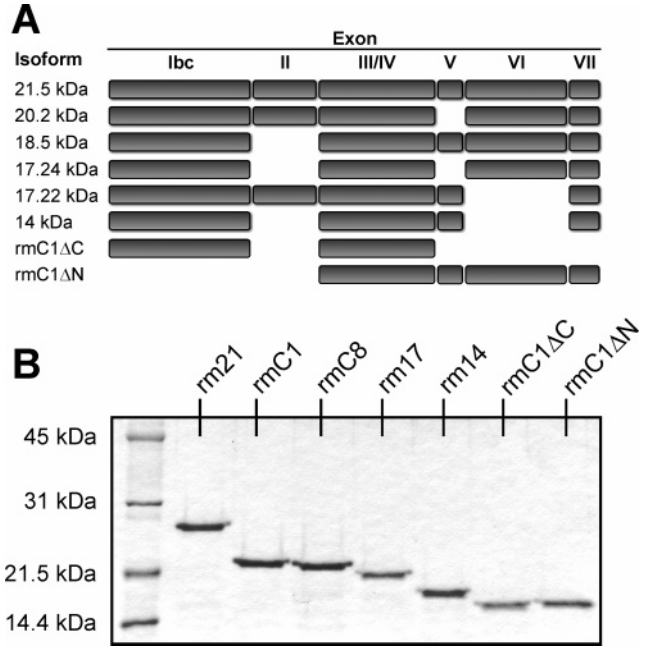


FIGURE 1: (A) Structure of the murine classic MBP gene, showing the exons that form each isoform. The human, bovine, and murine MBP genes are similarly structured; these alternately spliced products are spatially targeted, and their occurrence is developmentally regulated. Here, recombinant forms of the 21.5 kDa (rm21), 18.5 kDa (rmC1 and rmC8), 17.22 kDa (rm17), and 14 kDa (rm14) isoforms have been studied, in addition to N- and C-terminal deletion mutants of the 18.5 kDa isoform (rmC1ΔN and rmC1ΔC, respectively). Physical properties (number of residues, including the hexahistidine tag, and net charge at neutral pH) of these proteins are as follows: 202 and +23 for rm21, 176 and +19 for rmC1, 176 and +13 for rmC8, 160 and +19 for rm17, 135 and +15 for rm14, 121 and +11 for rmC1ΔN, and 111 and +12 for rmC1ΔC (*16*). Further diversification of the MBP family, especially of the best-studied 18.5 kDa isoform, is due to a plethora of post-translational modifications such as phosphorylation, deimination, and methylation (Table 1) (*9*, *12*, *41*). (B) SDS−PAGE of recombinant murine isoforms and deletion mutants. A 2 $\mu$g portion of protein was loaded in each lane, separated on a 12% polyacrylamide gel, and stained with Commassie R-250. Due to its highly cationic nature, MBP migrates more slowly on SDS−polyacrylamide gels than neutral proteins of comparable size.

alternate splicing to generate different isoforms (reviewed in ref *9*). The "classic" MBP gene arises from the third transcription start site of the Golli gene, and encodes products ranging from 14 to 21.5 kDa in size (Figure 1A). The best-studied splice isoform of this family is the 18.5 kDa MBP, since it is preponderant in adult human and bovine myelin. Further diversity of this MBP isoform is achieved by a plethora of post-translational modifications: N-terminal acylation, methylation, deamidation, phosphorylation, ADP ribosylation, and deimination (the irreversible enzymatic conversion of arginine to citrulline) (*9*, *10*). These changes result in the cumulative reduction of MBP's net positive charge, and a protein preparation from myelin can be separated by ion exchange chromatography into a series of charge components or isomers denoted C1−C8 (*11*, *12*). The least-modified form, C1, has a net charge of +19 at neutral pH, and predominates in normal adult myelin. The most-modified form, C8, has a net charge of +13 at neutral pH and is primarily deiminated. Intermediate forms are also deamidated and phosphorylated. MBP is a candidate autoantigen in multiple sclerosis, in which the proportion of deiminated isoform C8 is increased (*12*). The main function of the classic 18.5 kDa MBP is to hold the cytoplasmic leaflets of the oligodendrocyte membrane processes in close apposition, thus maintaining the structural integrity of the myelin sheath. Net charge reduction by post-translational modification attenuates this interaction. Myelin basic protein is a highly flexible and extended molecule, and belongs to the emerging "intrinsically unstructured" or "conformationally adaptable" class that is now known to comprise several hundred proteins, including tau and MAP2 (*9*, *13*).

Several lines of evidence implicate the MBPs as additional regulators of the cytoskeleton in addition to their main function of maintaining the spacing of myelin lamellae. First, MBP interacts in a $Ca^{2+}$-dependent manner with calmodulin (*14*), and polymerizes and bundles actin (*15*, *16*). Both associations are modulated by post-translational modifications. Second, MBP was identified in crude extracts of rat brain using the STOP (stable tubule only polypeptide) assay through its ability to protect microtubules from cold-induced depolymerization (*17*). Numerous MAPs are present in the brain, but MBP was one of only two proteins identified by this sensitive assay; moreover, the interaction appeared to be regulated by $Ca^{2+}$-bound calmodulin (*17*). Myelin basic protein has also been shown to be copurified with tubulin and actin upon detergent extraction of the myelin membrane (*18*), and to colocalize with CNP and microtubules in the processes of cultured myelinating oligodendrocytes (*19*, *20*). Oligodendrocytes isolated from *shiverer* transgenic mice, which lack all but the first two exons of the classic MBP gene, exhibit aberrant morphologies in culture which are due to underlying defects in cytoskeletal organization (*21*). A signal transduction pathway that results in microtubule depolymerization within cultured myelin sheaths is also dependent on the presence of MBP (*22*), and can be recovered in *shiverer* mice by the introduction of MBP transgenes (*23*). This pathway is in part mediated by the clustering of galactocerebrosides in the oligodendrocyte cell membrane in relation to underlying MBP domains (*24*).

Our knowledge of the nature of the MBP−tubulin interaction is currently limited. The earliest study on inhibition of tubulin carboxypeptidase activity (*25*) used MBP which had not been separated into charge isomers by cation exchange chromatography, and this MBP preparation was thus highly heterogeneous due to variations in the extent of post-translational modifications (reviewed in ref *9*). A later paper established the calmodulin-dependent ability of MBP to stabilize microtubules, and presented immunofluorescence microscopy data suggesting that MBP might be a microtubule bundling protein (*17*), though this MBP preparation was also unfractionated. Subtilisin-digested (S-tubulin) and control tubulin were stabilized by MAP2, histone H1, and (unfractionated) MBP to a similar extent, whereas tau stabilized S-tubulin significantly more than undigested tubulin, indicating that these basic proteins interact differently with tubulin (*26*).

In this study, we have used highly purified preparations of diverse splice isoforms, and charge components, of MBP, to characterize in detail this protein family's interaction with tubulin. Transmission electron microscopy (TEM) and light scattering were utilized to demonstrate directly that MBP can promote the polymerization of tubulin into microtubules under solution conditions which are not otherwise favorable

Table 1: Some Sites of Post-Translational Modification of the 18.5 kDa Isoform of Bovine MBP As Previously Determined by Mass Spectrometry of Tryptic Fragments by Zand et al. (*41*)[a]

| isomer | sites of modification |
|---|---|
| bC1 | N-terminal acylation |
| bC2 | deamidation, Q146 |
| bC3 | phosphorylation, T97 and S164 |
| bC4 | phosphorylation, S54, T97, and S160 |
| bC5 | phosphorylation, S7, S54, T97, and S164 |
| bC6 | phosphorylation, S7, S54, T97, S160, and S164 |

[a] The bC1 component (charge isomer) is the most cationic, with a net charge of +19 over 169 residues. Components bC2−bC6 are successively reduced in net positive charge. The bovine sequence numbering is given; a comparison with other 18.5 kDa MBP sequences is published elsewhere (*9*).

for assembly, and can induce the formation of microtubule bundles. The effects of both reversible and irreversible post-translational modifications and alternate splicing on the interaction of MBP with tubulin were also investigated.

## EXPERIMENTAL PROCEDURES

*Proteins*. Tubulin was purified from fresh bovine brain (Ontario Agricultural College, Guelph, ON) using the method of Castoldi and Popov (*27*). The tubulin concentration was determined using an extinction coefficient $\epsilon_{280}$ of 115 000 $M^{-1}$ $cm^{-1}$ (*28*), and the purity of tubulin preparations was assessed by SDS−polyacrylamide gel electrophoresis (PAGE). After preparation, small aliquots of concentrated tubulin were flash-frozen in liquid nitrogen and stored at −80 °C. For measurements of the critical concentration and GTPase activity, tubulin was purchased from Cytoskeleton Inc. (Denver, CO).

The term "MBP" is used here to refer, in general, to a member of the classic MBP family (Figure 1A). The natural protein, isolated from bovine brain, is called bMBP, and is predominantly the 18.5 kDa isoform, but comprises a mixture of charge isomers that must be further fractionated by ion exchange chromatography (*11*). Here, the charge isomers of 18.5 kDa bovine MBP (labeled bC1−bC6 in order of increasing level of post-translational modification and decreasing net positive charge, Table 1) were purified from the delipidated white matter of a 2-year-old steer brain, using acid extraction followed by cation exchange chromatography as previously described (*29*). (Adult bovine brain proffers very little of the deiminated bC8 charge component.) These proteins were a gift from D. Wood and M. Moscarello (Hospital for Sick Children, Toronto, ON).

Recombinant protein expressed in *Escherichia coli*, of the murine MBP gene, is termed here rmMBP. The rmMBP preparation of the 18.5 kDa isoform is post-translationally unmodified, and is thus an analogue of the least-modified natural C1 isoform; we here call it rmC1 (*30*). From rmC1, a mutant called rmC8 has been constructed by specific R/K → Q substitutions in an effort to study the effects of deimination, as occurs in the C8 component predominant in multiple sclerosis patients (*31*). Also from rmC1, both N-terminal and C-terminal deletion mutants, denoted rmC1ΔN and rmC1ΔC, respectively, have been constructed for the study of the functional roles of different segments (Figure 1) (*32*). Finally, expression constructs for the murine 14, 17.22, and 21.5 kDa MBP isoforms (Figure 1A) were a gift from A. Campagnoni and C. Campagnoni (Neuropsychiatric Institute, University of California, Los Angeles, CA) and are here termed rm14, rm17, and rm21, respectively.

All expression constructs consisting of cDNA for the murine 18.5 kDa isoform (rmC1, for recombinant murine C1), the quasi-deiminated form (rmC8), 14 kDa (rm14), 17.22 kDa (rm17), and 21.5 kDa (rm21) MBP isoforms, in addition to two terminal deletion mutants of the 18.5 kDa isoform (rmC1ΔC and rmC1ΔN), in pET22b(+) plasmid vectors (Novagen, Madison, WI) were transformed into *E. coli* BL21-CodonPlus(DE3)-RP (Stratagene, La Jolla, CA). These 18.5 kDa MBP variants were expressed and purified by nickel chelation chromatography as previously described (*16*, *30*−*32*).

All MBP concentrations were determined with a micro BCA assay (Pierce Biotechnology, Rockford, IL) using bC1 at a known concentration as a standard. All MBP preparations were routinely assessed by SDS−PAGE after purification (Figure 1B).

*Light Scattering*. Light scattering was used to monitor the assembly of tubulin by MBP. Samples (60 μL) of 20 μM tubulin solutions in G-PEM buffer [80 mM PIPES-KOH (pH 6.8), 0.5 mM $MgCl_2$, 1 mM EGTA, and 1 mM GTP] were loaded into a 3 mm × 3 mm quartz cuvette (Hellma Canada, Concord, ON), and light scattering was recorded at an angle of 90°. Scattering was monitored with a SPEX Fluorolog spectrofluorimeter (Spex Industries, Edison, NJ) set at an excitation wavelength of 340 nm with a bandwidth of 0.7 nm, and an emission wavelength of 340 nm with a bandwidth of 1.1 nm. Tubulin assembly was promoted by the addition of either MBP at various molar ratios or glycerol to a final concentration of 10%.

*Transmission Electron Microscopy (TEM)*. Assemblies of tubulin formed by MBP were prepared under the conditions described for light scattering experiments. Droplets (10 μL) of the MBP/tubulin solution were applied to 400 mesh Cu electron microscope grids supporting a thin layer of carbon film and incubated for 2 min. Excess solution was wicked off with filter paper, and 10 μL of 2% uranyl acetate stain was then applied to each grid. Stain was wicked off with filter paper after incubation for 2 min, and the grids were then allowed to air-dry for 15 min prior to TEM analysis. Electron micrographs of the samples were recorded on a Leo912AB TEM (Leo GmbH, Oberkochen, Germany), by direct digital image capture with an EsiVision CCD-BM/1k SSCCD camera, at nominal magnifications of 20000−40000×, and operating at 100 kV. Structures were considered to be representative of the sample when they could be observed at four separate locations on each of duplicate or triplicate grids.

*Critical Concentration*. Measurements of the critical concentration of tubulin were performed according to the method outlined by Lee and Timasheff (*33*). Light scattering measurements (see above) were performed on samples containing 2.5−10 μM tubulin and 1 μM bC1. All samples were dissolved in G-PEM assembly buffer and were incubated at 37 °C for 15 min. At least four different concentrations were measured in each experiment, and experiments were performed in triplicate; linear regression analysis was performed, and the *x*-intercepts of these fits were designated the tubulin critical concentration.

*GTPase Activity*. Measurements of tubulin GTPase activity upon polymerization were performed using an EnzChek Phosphate Assay Kit (Molecular Probes, Eugene, OR) that was adapted for use in a 96-well microplate. Samples were prepared so that they contained either 20 $\mu$M tubulin and 2.5 $\mu$M bC1, 20 $\mu$M tubulin, or 2.5 $\mu$M bC1. The release of inorganic phosphate ($P_i$), which is indicative of GTPase activity, was monitored by the conversion of 2-amino-6-mercapto-7-methylpurine riboside (MESG) to ribose 1-phosphate and 2-amino-6-mercato-7-methylpurine by purine nucleoside phosphorylase (PNP). With this system, the increase of absorbance at 360 nm is directly related to the release of $P_i$. To control for $P_i$ contamination in the reagents, the EnzChek kit was used as a $P_i$ "mop" where all reagents were combined and allowed to incubate for 10 min at 22 °C before the addition of tubulin. The samples were heated to 37 °C, and a baseline measurement was taken (for use as the background blank). To control for the scattering effects of tubulin polymerization at 360 nm, a sample containing all the reagents except MESG was measured in parallel and subsequently subtracted from the tubulin-containing samples at each time point. Measurements were taken on a SpectraMax 340PC microplate reader controlled by SoftMaxPro version 3.1 (Molecular Devices Corp., Sunnyvale, CA) at 5 min intervals.

*Sedimentation Assay.* Tubulin pelleting assays, based on the method of Kar et al. (*34*), were used to test the effect of paclitaxel on MBP binding. Briefly, different concentrations of bC1 were incubated with 5 $\mu$M tubulin in G-PEM buffer containing 5% dimethyl sulfoxide (DMSO, from Sigma-Aldrich, Oakville, ON), at 37 °C for 20 min, and then subjected to centrifugation at 100000*g* for 40 min at 37 °C. Duplicate experiments were performed with the inclusion of 40 $\mu$M paclitaxel (Sigma-Aldrich).

After centrifugation, the top 100 $\mu$L of each 200 $\mu$L sample was removed with a syringe and mixed with 25 $\mu$L of 5× SDS−PAGE loading buffer [60 mM Tris-HCl (pH 6.8), 25% glycerol, 2% sodium dodecyl sulfate, 14.4 mM 2-mercaptoethanol, and 0.1% bromophenol blue]. A 25 $\mu$L portion of 5× SDS−PAGE loading buffer was added to the remaining 100 $\mu$L in the centrifuge tube, and the mixture was used to wash the bottom of the tube vigorously to recover pelleted protein. Samples (10 $\mu$L) of both the pellet and supernatant were analyzed using SDS−PAGE with a resolving acrylamide concentration of 12%, and staining with Coomassie R-250. The program Scion Image (Scion Corp., Frederick, MD) was used to quantify the densities of protein bands. The fraction of MBP bound to tubulin was calculated as the density of the pellet MBP band, corrected for the density of the MBP supernatant band, divided by the sum of the densities of the supernatant and pellet bands.

*Preparation of Tubulin Sheets.* Sheets of crystalline tubulin were prepared using the method of Hoenger et al. (*35*). Briefly, 10 $\mu$M tubulin in 80 mM PIPES-KOH (pH 6.8), 2 mM GTP, 2 mM $MgCl_2$, and 15% DMSO was incubated at 37 °C for 30 min. The resulting assemblies, a mixture of microtubules and tubulin sheets, were stabilized by the addition of concentrated paclitaxel (in DMSO) to a final concentration of 20 $\mu$M. Paclitaxel-stabilized tubulin structures, in the presence and absence of bC1, were negatively stained for TEM as described above.

## RESULTS

*Tubulin Polymerization by the Most Highly Cationic Charge Component of 18.5 kDa Bovine MBP (bC1).* An early study described a dose-dependent increase in the turbidity of tubulin solutions upon addition of unfractionated MBP (heterogeneous mixture of modified forms), but did not address the nature of the resultant complexes (*25*). Here, we first used a homogeneous preparation of the most cationic charge isomer of natural 18.5 kDa bovine MBP, bC1, as the archetype of the family. Light scattering was used to track the assembly of 20 $\mu$M tubulin at 37 °C. In the buffer that was used, this concentration of tubulin is lower than the critical concentration for spontaneous assembly, and microtubule growth will not occur under these conditions without an additional polymerizing agent (*36*). In these experiments, the baseline was always the same (negligible scattering by tubulin alone), and the addition of MBP promoted a rapid assembly. At the lowest concentrations of MBP that were tested, 1:16 and 1:8 bC1:tubulin molar ratios, the character of the scattering trace was similar to that of a glycerol control, in that a short lag phase was succeeded by a rapid increase in scattering followed by a plateau (Figure 2A). At higher ratios of bC1 to tubulin, no lag phase was observed, and in an equimolar mixture of bC1 and tubulin, a large initial increase in turbidity was followed by decay to a lower final value. The high initial spike in scattering intensity at high MBP concentrations is reminiscent of the overshoot observed at high tubulin concentrations (*36*).

A duplicate experiment at the 1:8 bC1:tubulin molar ratio was used to generate a time series of samples for analysis by TEM. Small volumes were removed from the reaction mixture immediately prior to the addition of bC1, and 1, 2, 5, and 10 min after addition, and then treated with uranyl acetate to fix the samples (*37*). No tubulin organization was observed prior to the addition of bC1 (Figure 2B), but filamentous structures were observed as early as 1 min after addition of bC1 (Figure 2C). After 2 min, numerous fully assembled microtubules were observed, and many thinner filaments, which may represent intermediates in microtubule assembly, were also present (Figure 2D). These filaments were less prevalent at 5 min (Figure 2E) and 10 min (Figure 2F), and many microtubules were observed to be associated into bundles. A sample was taken at the 1 min point for analysis by a TEM from a polymerization trial with a 1:1 bC1:tubulin molar ratio (Figure 2G). Numerous tubulin ring structures were observed in this sample, many of which appeared to be double rings.

The micrographs presented in Figure 2 indicate that MBP can promote both the polymerization of $\alpha\beta$-tubulin dimers into microtubules and the further assembly of these microtubules into bundles. To explore the bundling ability of MBP further, bC1 was added in a 1:4 MBP:tubulin molar ratio to microtubules prepolymerized in the presence of 10% glycerol at 37 °C. After bC1 addition, an approximately 3.5-fold increase in scattering was observed, and the final value of scattering was substantially higher than that observed for a duplicate sample of tubulin treated with the same amount of bC1 in the absence of glycerol (Figure 3A). TEM of samples collected at the indicated points confirmed substantial bundling of tubulin by bC1 in the presence and absence

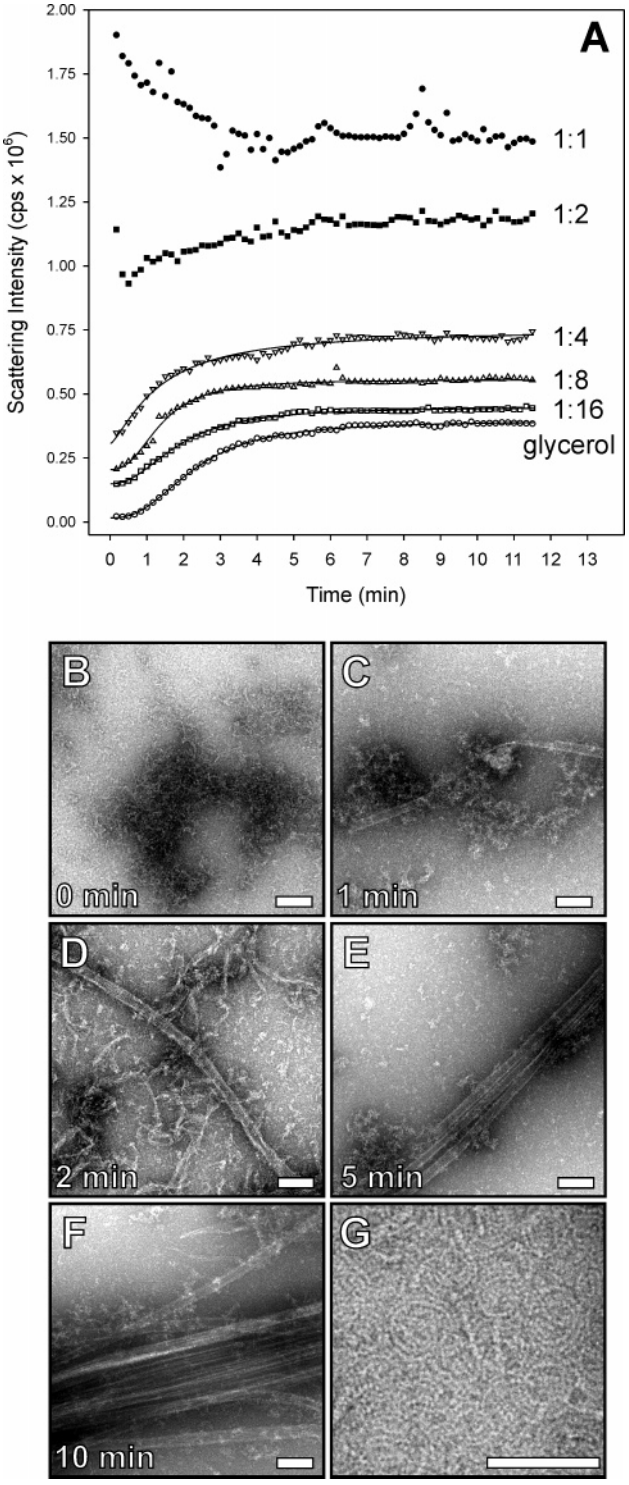


FIGURE 2: Assembly of tubulin by unmodified 18.5 kDa bovine MBP. (A) Assembly of 20 $\mu$M tubulin promoted by bC1, at various molar ratios, or by 10% glycerol (final concentration), monitored by 90° light scattering. (B−F) Negatively stained samples of a parallel polymerization experiment performed at a bC1:tubulin ratio of 1:8, visualized with TEM. Scale bars are 100 nm. (G) Tubulin ring structures observed 1 min after the addition of bC1 to tubulin at a 1:1 molar ratio, negatively stained, and visualized with TEM. The scale bar is 50 nm.

of glycerol (Figure 3C,D), and the absence of bundling in samples polymerized by glycerol alone (Figure 3B).

The critical tubulin concentration in the presence of 1 $\mu$M bC1 was determined to be 0.69 $\pm$ 0.05 $\mu$M (Figure 4A). This value compares favorably with the value of 0.91 $\mu$M

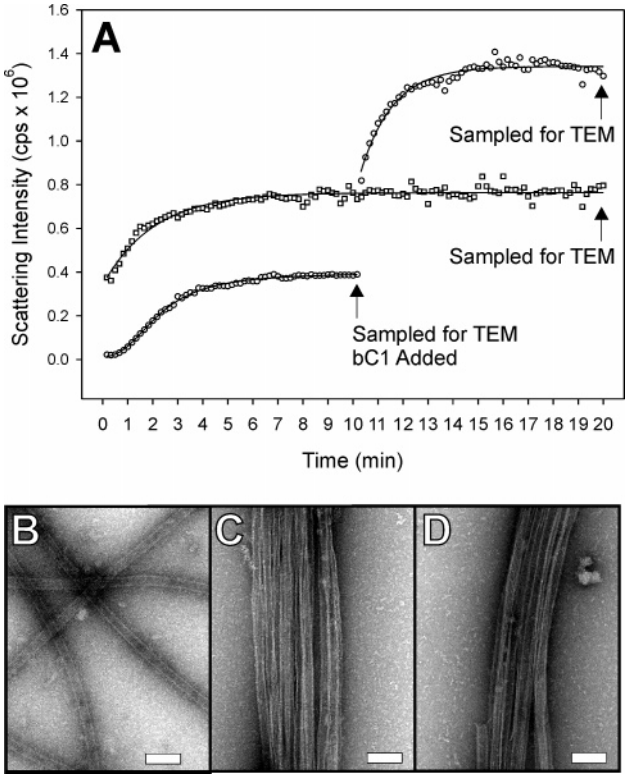


FIGURE 3: Bundling of microtubules by unmodified 18.5 kDa bovine MBP (bC1). (A) Assembly of 20 $\mu$M tubulin promoted by bC1 (□), at a molar ratio of 1:4 (MBP:tubulin), or by glycerol, to a final concentration of 10%, followed by the addition of bC1 to a molar ratio of 1:4 (○). (B−D) Negatively stained preparations of samples taken at indicated points. Scale bars are 100 nm. (B) Microtubules formed by glycerol alone. (C) Bundles of microtubules, initially formed by glycerol, observed after the addition of bC1. (D) Bundles observed in the presence of bC1 but in the absence of glycerol.

in the presence of 0.8 $\mu$M tau (*38*), and 0.45 $\mu$M in saturating concentrations of MAP2 (*39*), both of which represent "specific" tubulin polymerizers. The critical concentration of tubulin in the absence of either bC1 or glycerol was assumed to be >20 $\mu$M, since no appreciable increase in scattering intensity was recorded under these conditions in a parallel experiment (results not shown), again in agreement with previous observations (*33*, *36*, *40*). The GTPase activity associated with tubulin assembly was significantly enhanced in the presence of bC1, compared to that with tubulin alone, whereas bC1 alone did not demonstrate any GTPase activity (Figure 4B). Thus, the tubulin is polymerizing and not simply aggregating in the presence of MBP, as already indicated by the TEM data (Figure 2D−F).

*Comparison of Classic MBP Splice Isoforms.* Recombinant murine (rm) MBPs were used to test the ability of the classic isoforms to assemble tubulin, because the natural forms of these splice variants are difficult to isolate from central nervous system myelin in appreciable quantities (Figure 1). The isoforms represented here include recombinant forms of the murine 21.5, 17.22, and 14 kDa variants (denoted rm21, rm17, and rm14, respectively) in addition to rmC1 (the murine 18.5 kDa variant), which was used rather than bC1 to control for the presence of the C-terminal hexahistidine tag present on all recombinant forms (*16*). The activities of the terminal deletion mutants of rmC1, denoted rmC1$\Delta$C and rmC1$\Delta$N (*32*), were also used, as was rmC8,

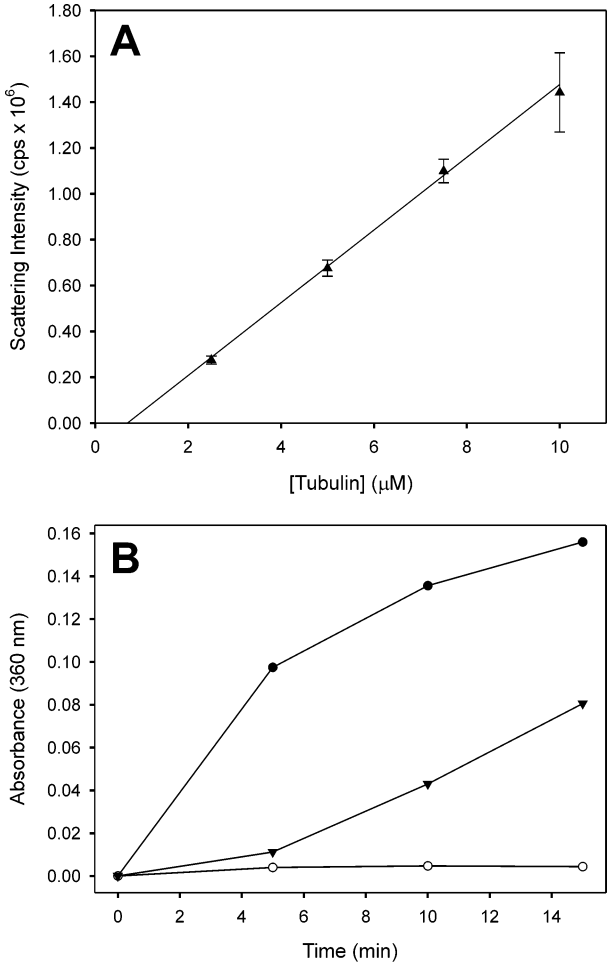


FIGURE 4: (A) Measurements of critical tubulin concentrations in the presence of 1 $\mu$M unmodified 18.5 kDa bovine MBP (bC1). Light scattering data at 340 nm were collected at 37 °C in the presence of 1 mM GTP, and the plateau values were plotted vs the various tubulin concentrations. Shown are the results from three separate experiments; linear regression of the average values extrapolates to a critical tubulin concentration of 0.69 ± 0.05 $\mu$M. (B) Measurements of tubulin GTPase activity in the absence and presence of bC1. GTPase activity was determined by the rate of release of $P_i$, which was monitored by the conversion of 2-amino-6-mercapto-7-methylpurine riboside to ribose 1-phosphate and 2-amino-6-mercato-7-methylpurine, which has an absorbance maximum of 360 nm. Under favorable assembly conditions, 20 $\mu$M tubulin was added to samples containing either 2.5 $\mu$M bC1 (●) or an equivalent volume of buffer (no bC1, ▼). Microtubules assembled in the presence of bC1 exhibit significantly higher GTPase activity than microtubules assembled in its absence. Alone, bC1 did not exhibit any intrinsic GTPase activity (○).

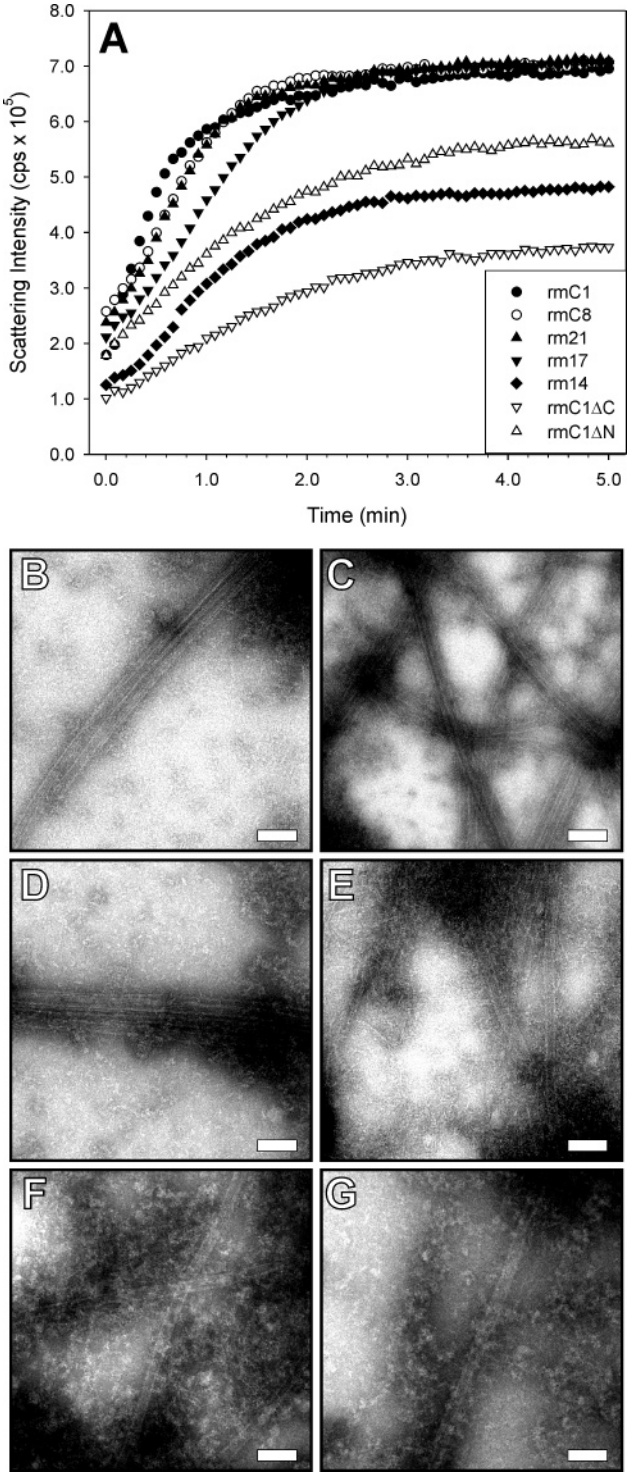


FIGURE 5: Assembly of tubulin by recombinant murine isoforms of myelin basic protein. (A) Assembly of 20 $\mu$M tubulin promoted by classic splice isoforms (21.5, 17.22, and 14 kDa) of MBP, and N- and C-terminal deletion mutants of the 18.5 kDa isoform, at molar ratios of 1:8 (MBP:tubulin) monitored by 90° light scattering. (B−G) Negatively stained samples of parallel polymerization experiments harvested 10 min after the addition of MBP to tubulin: (B) rm21 (21.5 kDa), (C) rmC1 (18.5 kDa), (D) rm17 (17.22 kDa), (E) rm14 (14 kDa), (F) rmC1ΔC, and (G) rmC1ΔN. Scale bars are 100 nm.

a reduced charge mutant of rmC1 designed to mimic the effects of deimination, an irreversible post-translational modification associated with multiple sclerosis (*31*).

The tubulin-assembling activities of the isoforms were assayed as for the charge isomers, using 90° light scattering with an MBP:tubulin molar ratio of 1:8 (Figure 5A). The final extent of tubulin assembly induced by rm21 and rm17 was similar to that induced by rmC1. Additionally, the reduced charge mutant rmC8 was able to induce an amount of tubulin assembly comparable to that of rmC1, its unmodified analogue. The rm17 variant polymerized tubulin at a slightly slower rate than rm21 and rmC8, both of which were slightly slower than rmC1. Overall reductions in tubulin assembly ability (rate and final extent), compared to that of rmC1, were observed for rm14 and both deletion mutants. Transmission electron microscopy was used to determine the effect of alternate splicing and deletions on the tubulin structures formed. In samples of tubulin assembled by rm21

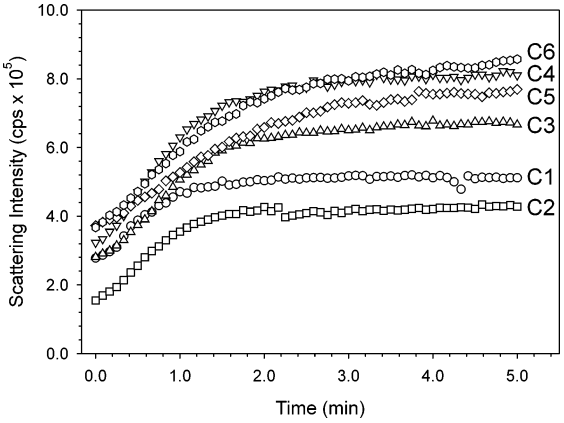


FIGURE 6: Assembly of tubulin by charge isomers of 18.5 kDa bovine MBP. Assembly of 20 $\mu$M tubulin promoted by charge isomers (post-translationally modified components) of 18.5 kDa bovine MBP (bC1−bC6), at molar ratios of 1:8 (MBP:tubulin) monitored by 90° light scattering.

(Figure 5B), rmC1 (Figure 5C), and rm17 (Figure 5D), numerous microtubules, which were frequently assembled into bundles, were observed. In samples of tubulin with rm14 (Figure 5E), rmC1ΔC (Figure 5F), and rmC1ΔN (Figure 5G), fewer microtubules were present and bundling was not observed. However, the samples produced using rm14 appeared to contain numerous short filaments that were not observed in the samples produced using the deletion mutants.

*Comparison of Post-Translationally Modified Charge Isomers (Components) bC1−bC6 of 18.5 kDa Bovine MBP*. Charge isomers of 18.5 kDa MBP isolated from bovine brain were compared with respect to their ability to assemble tubulin. These isomers are labeled bC1−bC6 in order of increasing level of post-translational modification and, thus, decreasing net positive charge (Table 1). Bovine rather than murine natural charge isomers were used due to the substantially larger amount of MBP available from a single bovine brain, which, however, yields very little of the deiminated bC8 charge isomer. Combinations of post-translational modifications, such as deamidation and phosphorylation, have been identified in the bC1−bC6 components by mass spectrometry (*12*, *41*). Here, light scattering assays indicated that bC2, subject only to deamidation, had a somewhat weakened ability to assemble tubulin. The more highly modified forms bC3−bC6, which are also phosphorylated, had better tubulin assembling ability when compared to unmodified bC1 (Figure 6). As for the recombinant variants, these natural forms of the protein promoted both polymerization and bundling of tubulin, the latter of which was confirmed by TEM (results not shown).

*Effects of Paclitaxel, and Cocrystallization of MBP and Tubulin.* The effect of paclitaxel on the ability of bC1 to bind to tubulin was tested as a preliminary to cocrystallization trials of bC1 with paclitaxel-stabilized crystalline sheets of tubulin. The results of cosedimentation trials of bC1 and tubulin are shown in Figure 7; only tubulin which has been assembled into microtubules sediments under these experimental conditions. No differences in the partitioning of bC1 between the sedimented and solution portions of the samples were seen between samples containing and lacking paclitaxel. The only observable effect of the paclitaxel was to ensure complete polymerization at MBP concentrations that were too low to assemble all the tubulin fully. Crystalline sheets

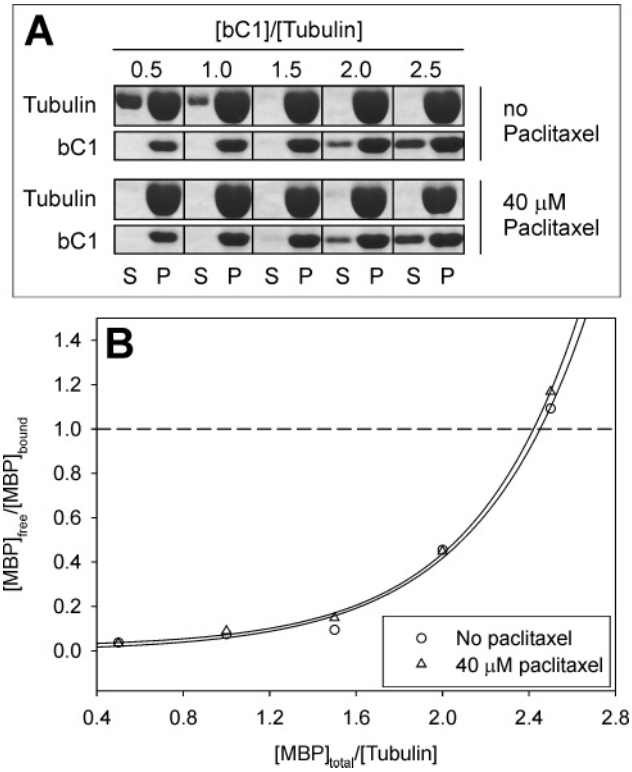


FIGURE 7: Assembly of tubulin by unmodified 18.5 kDa bovine MBP (bC1) in the presence and absence of paclitaxel. (A) SDS−PAGE analysis of cosedimentation assays for the binding of bC1 to tubulin. Samples loaded in S (supernatant) lanes were taken from the top half of the sample after centrifugation and P (pellet) lanes from the bottom. (B) Ratio of free and bound MBP determined by densitometry of gels in panel A. The horizontal line indicates the point at which the amounts of free and bound MBP are equal.

of tubulin were readily formed in the presence of 15% DMSO and 20 $\mu$M paclitaxel; Figure 8A depicts both a microtubule and a large, planar sheet of tubulin formed under these conditions. However, the addition of bC1 to preformed sheets of tubulin (1:4 MBP:tubulin molar ratio) resulted in bundling and disruption of these sheets (Figure 8B,C).

## DISCUSSION

*Assembly of Tubulin by MBP*. In cultured oligodendrocytes, MBP colocalizes with tubulin (*19*, *20*). In a sensitive STOP assay, MBP was identified as one of two brain proteins that acted as a $Ca^{2+}$-bound calmodulin regulated "superstabilizer" of microtubules, which the authors considered physiologically significant (*17*, *42*). These and other in vivo observations (*21*−*23*) collectively suggest a strong and specific interaction between MBP and tubulin, which has yet to be characterized fully. Unfractionated MBP, comprising a mixture of charge isomers derived from differing degrees of post-translational modification, has previously been shown to induce the association of tubulin in vitro (*25*). It has since been shown that post-translational modifications of MBP can modify its associations with numerous ligands, including lipids (*11*, *43*, *44*), itself (*45*, *46*), calmodulin (*14*, *47*), and actin (*15*, *16*). In this study, fractionated natural bovine MBP charge components, and recombinant murine forms expressed in *E. coli*, have been used to study the specific roles that post-translational modification and alternate splicing may play in regulating the interaction of MBP and tubulin.

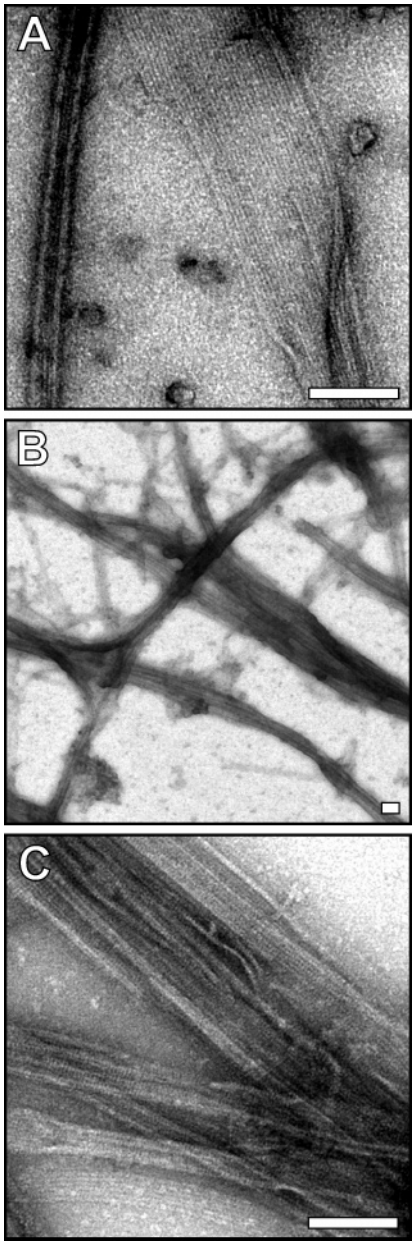


FIGURE 8: Interaction of MBP with paclitaxel-stabilized crystalline sheets of tubulin. (A) Structures produced by polymerization of tubulin with DMSO followed by treatment with paclitaxel. Both microtubules (left) and planar sheets (right) were observed. (B and C) Planar sheets from panel A treated with bC1 at a 1:4 (MBP:tubulin) molar ratio. All scale bars are 100 nm.

The highly cationic, unmodified bC1 charge isomer of 18.5 kDa MBP caused rapid assembly of tubulin, even at relatively low MBP:tubulin molar ratios (1:16). The electron micrographs presented herein (Figure 2) are the first direct visualizations of microtubule structures formed by MBP. At intermediate MBP:tubulin molar ratios (1:8 and 1:4), the lag phase of tubulin polymerization, associated with the formation of tubulin nuclei, was abolished. This phenomenon is very similar to that observed for actin polymerization modulated by MBP (*15*, *16*, *48*), and suggests that MBP can facilitate rapid tubulin nucleation, expediting this rate-limiting step. At the highest molar ratio that was tested (1:1 MBP:tubulin), the character of the light scattering trace changed, starting high and decaying to an equilibrium value, a phenomenon that has been observed previously (*36*). TEM of a negatively stained sample taken at the minute mark of this experiment showed that numerous tubulin rings were present (Figure 2G), structures that were not observed at the same time point in the polymerization experiment performed at a 1:8 molar ratio (Figure 2C). Moreover, the rings appeared to be doubled, similar to ones recently observed in experiments demonstrating that tau can polymerize tubulin under conditions which do not otherwise favor assembly (*49*). It is possible that different assembly intermediates are favored at different ratios of MBP to tubulin, as primarily filamentous intermediates were observed in the time course experiment at a 1:8 MBP:tubulin molar ratio. The ring structures may also represent an underlying polymerization−depolymerization phenomenon (*50*), as suggested by the somewhat oscillatory behavior of the scattering intensities (*51*).

*Effects of Alternate Splicing*. The classic splice isoforms containing exon II of the classic MBP gene (the 21.5 and 17.22 kDa isoforms) are known to be closely associated with tubulin in vivo (*52*−*54*). Here, rm21 appeared to assemble tubulin in a manner (rate and final extent) similar to that of 18.5 kDa isoform rmC1, which lacks the exon II-derived region, whereas rm17 polymerized tubulin at a slower initial rate than either rm21 or rmC1 (Figure 5A). Parallel TEM experiments showed that these isoforms all had the capacity to bundle microtubules (Figure 5B−D). It has previously been hypothesised that a highly conserved KPGFG motif in the exon VI-derived region of classic MBP, which is similar to the KPGGG tubulin-binding motif in tau, is a primary site for the binding of MBP to tubulin (*55*). Our data do not support this hypothesis, as the rm17 variant lacks the region derived from exon VI. Indeed, the replacement of a glycine in the tau motif with a phenylalanine in the MBP motif cannot be considered to be a conservative substitution. Thus, although this motif may be involved in binding tubulin, it is not the only region of MBP to do so. Of more relevance are the common physicochemical properties of these proteins (MBP, tau, and MAP2): conformational adaptability, extensive modification, and multifunctionality, as discussed below.

The final extent of light scattering, a measure of both tubulin polymerization and bundling, induced by rm14, rmC1ΔC, and rmC1ΔN was lower than that induced by the remaining isoforms. TEM confirmed that these variants were able to promote microtubule polymerization; however, microtubules were less abundant, and bundling was not observed. The rm14 isoform and the rmΔN and rmΔC deletion mutants are substantially shorter than the 21.5, 18.5, and 17 kDa variants (Figure 1), indicating they may not be long enough to serve as an effective bridge between microtubules. If a primary and/or essential tubulin-binding motif exists in MBP, it must reside in the region derived from exons III and IV of the classic gene, the only region of commonality shared by all splice isoforms that were tested. In rodents (mice and rats), the 14 kDa isoform predominates in adult myelin. Here, rm14 appeared to polymerize tubulin more slowly than rmC1, and to a lesser final extent with no (or significantly less) bundling. However, different splice isoforms can associate with tubulin in myelin in a developmentally and spatially regulated manner.

*Effects of Post-Translational Modifications on Tubulin Assembly by MBP*. Intriguingly, there was no attenuation in the ability of rmC8 to assemble tubulin compared to that of

rmC1, its unmodified analogue (Figure 5). This result stands in contrast to that observed for actin, as it was seen that amino acid replacements mimicking deimination attenuated the ability of MBP to assemble actin (*15*), and suggests that the interaction between MBP and tubulin entails specificity and is not solely dependent on net charge. The removal of the acidic carboxy-termini of tubulin by digestion with subtilisin has been shown elsewhere not to alter the stabilization of tubulin by MAP2, but did with tau (*26*). In that investigation, the basic proteins histone H1 and an unfractionated MBP preparation were used as controls and behaved like MAP2. As for MAP2, it can be concluded here that associations of the acidic carboxy termini of tubulin are not the primary determinant of the interaction, although they are not necessarily ruled out.

Further assembly experiments using charge isomers of 18.5 kDa bovine MBP revealed a striking divergence of the influence of post-translational modifications on the ability of MBP to assemble actin and tubulin (Figure 6). The bC2 component, identical to bC1 save for deamidation at Gln146 (Table 1), showed an attenuated ability to assemble tubulin, consistent with the attenuated ability of bC2, relative to bC1, to polymerize actin and bundle the microfilaments (*16*). However, the charge isomers with increasing reductions in net positive charge, bC3−bC6, exhibited enhanced ability to assemble tubulin when compared to bC1, the opposite to their effect on actin assembly (*16*). Indeed, the mostly highly modified bC4−bC6 induced the greatest extent of tubulin assembly, and so the interaction of MBP with tubulin cannot be described simply in terms of net charges and electrostatic attraction alone. We posit that phosphorylation of MBP is also an important determinant in this interaction, and explore this idea further.

These results with MBP present a contrast with MAP2, the predominant microtubule-associated protein found in brain, which exhibits attenuated microtubule association upon phosphorylation (*56*−*59*) and which is also intrinsically unstructured (*60*) and a target for calmodulin binding (*61*). Many studies have observed that phosphorylation attenuates the ability of tau (*62*, *63*), another intrinsically unstructured protein, to interact with tubulin, and this behavior was attributed to a reduction in cationicity. However, more recent studies have shown that certain patterns of tau phosphorylation have no effect on tubulin interaction (*64*), and that some phosphorylation events actually promote interaction with tubulin (*65*). Thus, site-specific phosphorylation and dephosphorylation of MBP may be a mechanism for either enhancing or attenuating the interaction with tubulin, as is the case with tau and MAP2 (*66*).

When oligodendrocytes extend processes, i.e., when microtubules are actively growing, MBP becomes phosphorylated by protein kinase C (*67*). Phosphorylation is known to stabilize α-helices in tau (*68*), and $\beta$-structures in MBP (*69*, *70*), and so may also stabilize predicted transient α-helices in MBP (*71*, *72*). This idea is in concordance with recent studies describing local "residual" structures in intrinsically unstructured proteins, including MAP2, which are regions of conformational preference for secondary structural elements which do not fully form in the absence of a binding partner (*60*, *73*, *74*). Phosphorylation of MBP may result in local secondary structural transitions in regions involved in interactions with tubulin. Thus, the addition of negatively charged moieties with concomitant conformational changes, and not a mere reduction of net positive charge, may explain the enhanced MBP−tubulin interaction observed in vitro with these charge components. Intriguingly, it has been shown that trimethylamine *N*-oxide (TMAO), an osmolyte which can stabilize structures in intrinsically unstructured proteins which are normally only formed upon association with binding partners, can enhance the ability of tau to assemble microtubules and also reverse the inhibition of assembly resulting from phosphorylation (*38*, *40*, *75*). This observation suggests that the attenuation of tubulin binding ability upon tau phosphorylation may also result from changes in local secondary structure.

*Tubulin and Actin Polymerization and Bundling by MBP*. As one point of commonality between the interaction of MBP with actin and tubulin, preformed microtubules were bundled to a greater extent by a given quantity of bC1 than the same amount of unpolymerized tubulin, indicating that a greater extent of bundling can be achieved when the MBP does not also need to maintain the integrity of the individual microtubules. This result is similar to that observed for bundling of F-actin by charge isomers bC1−bC6 of 18.5 kDa bovine MBP, all of which were able to promote comparable actin bundling despite having different abilities to polymerize G-actin into filaments (*16*).

The decrease in the extent of assembly of actin and the increase in the extent of assembly of tubulin resulting from an increasing level of post-translational modification of MBP, coupled with the proximity of all three molecules in the membrane processes of developing myelin, or the radial component of mature central nervous system myelin, may mean that modifications such as phosphorylation can cause switching of MBP from actin to tubulin. A similar mechanism has been described in neuronal cells for MAP2c, but in reverse, in that phosphorylation was seen to dissociate MAP2c from microtubules and localize it to peripheral membrane ruffles enriched in actin (*76*). This could potentially explain the depolymerization of tubulin, suggested to be mediated by MBP, that is observed upon the binding of antiGalCer antibodies to galactocerebrosides in the myelin membrane (*22*, *23*, *66*). This binding may be the first step in a signal transduction cascade that ultimately results in MBP dephosphorylation, possibly by triggering an influx of $Ca^{2+}$ (*77*). Support for this concept also arises in the observation that phosphorylated MBP is associated with detergent-resistant membrane microdomains (lipid rafts), putative signaling platforms, in adult myelin (*78*).

The fact that paclitaxel does not compete with bC1 for binding to tubulin (Figure 7) suggested that paclitaxel-stabilized crystalline tubulin sheets could be suitable crystallization substrates for MBP. Unfortunately, the addition of bC1 to planar tubulin sheets resulted in bundling and warping of these structures (Figure 8), and no assemblies suitable for crystallographic structural studies were observed (*9*, *45*, *46*).

*Role of MBP in Maintaining Cytoskeletal Organization in Myelin*. Central nervous system myelin is formed by the extension of membranous cellular processes from oligodendrocytes (*1*, *2*, *5*, *7*). The movement of the leading edge of these processes is driven first by actin polymerization (*18*), with subsequent stabilization by microtubule infiltration (*5*). One prominent myelin protein, CNP, has been shown to

mediate F-actin and microtubule organization in process outgrowth (*8*). MBP is also a prominent protein in late-developing and mature myelin, and has also been shown to interact with cytoskeletal proteins both in vivo (*17*−*20*, *42*), as part of galactocerebroside-mediated signal transduction pathways (*22*, *24*, *79*−*82*), and in vitro under $Ca^{2+}$-bound calmodulin regulation (*9*, *15*, *16*, *25*, *48*). During myelinogenesis, an actin-mediated event, MBP may function as an effector of process extension by stabilizing microfilaments. In mature myelin, MBP appears to serve as a link between actin filaments or bundles and the oligodendrocyte membrane (*83*). Our work here extends the roles of MBP to include microtubule stabilization in mature myelin. In particular, MBP could serve to cobundle actin and tubulin in the radial component of myelin, analogous to what has been observed for the microtubule-associated proteins MAP2 and tau (*84*).

## CONCLUSIONS

We have shown that the classic 18.5 kDa isoform of myelin basic protein polymerizes tubulin and bundles microtubules in a dose-dependent manner. Net positive charge reduction due to post-translational modifications (such as deamidation and phosphorylation) of MBP strengthened its ability to assemble tubulin, whereas charge reduction due to quasi-deimination had little effect compared to the unmodified protein. These results stand in contrast to the diminution of MBP's ability to assemble actin as a result of post-translational modifications that reduce the net positive charge. Thus, the interaction between MBP and tubulin may be modulated by site-specific modifications, potentially with concomitant changes in local structure. Since the segments derived from exons III and IV of the classic MBP gene were the only ones common to all MBP isoforms that were examined, they are likely to comprise putative tubulin-binding motifs. Since the MBP−cytoskeleton interactions have been shown to be regulated by $Ca^{2+}$−calmodulin binding, and by post-translational modifications, MBP could conceivably serve as another point of intersection in phosphorylation- and CaM-mediated signal transduction pathways controlling cytoskeletal architecture and stability in oligodendrocytes.

## ACKNOWLEDGMENT

We thank Drs. Denise Wood and Mario Moscarello (Hospital for Sick Children) for providing the bC1−bC6 charge isomers of bovine MBP, Drs. Celia and Anthony Campagnoni (Neuropsychiatric Institute, University of California) for expression constructs for recombinant forms of the 14, 17.22, and 21.5 kDa isoforms of murine MBP, and Dr. Joan Boggs (Hospital for Sick Children) for helpful discussions.

## REFERENCES

1. Baumann, N., and Pham-Dinh, D. (2001) Biology of oligodendrocyte and myelin in the mammalian central nervous system, *Physiol. Rev. 81*, 871−927.
2. Song, J., Goetz, B. D., Baas, P. W., and Duncan, I. D. (2001) Cytoskeletal reorganization during the formation of oligodendrocyte processes and branches, *Mol. Cell. Neurosci. 17*, 624−636.
3. LoPresti, P., Szuchet, S., Papasozomenos, S. C., Zinkowski, R. P., and Binder, L. I. (1995) Functional implications for the microtubule-associated protein tau: Localization in oligodendrocytes, *Proc. Natl. Acad. Sci. U.S.A. 92*, 10369−10373.
4. Richter-Landsberg, C., and Gorath, M. (1999) Developmental regulation of alternatively spliced isoforms of mRNA encoding MAP2 and tau in rat brain oligodendrocytes during culture maturation, *J. Neurosci. Res. 56*, 259−270.
5. Richter-Landsberg, C. (2000) The oligodendroglia cytoskeleton in health and disease, *J. Neurosci. Res. 59*, 11−18.
6. Muller, R., Heinrich, M., Heck, S., Blohm, D., and Richter-Landsberg, C. (1997) Expression of microtubule-associated proteins MAP2 and tau in cultured rat brain oligodendrocytes, *Cell Tissue Res. 288*, 239−249.
7. Richter-Landsberg, C. (2001) Organization and functional roles of the cytoskeleton in oligodendrocytes, *Microsc. Res. Technol. 52*, 628−636.
8. Lee, J., Gravel, M., Zhang, R., Thibault, P., and Braun, P. E. (2005) Process outgrowth in oligodendrocytes is mediated by CNP, a novel microtubule assembly myelin protein, *J. Cell Biol. 170*, 661−673.
9. Harauz, G., Ishiyama, N., Hill, C. M., Bates, I. R., Libich, D. S., and Farès, C. (2004) Myelin basic protein: Diverse conformational states of an intrinsically unstructured protein and its roles in myelin assembly and multiple sclerosis, *Micron 35*, 503−542.
10. Wood, D. D., and Moscarello, M. A. (1997) Molecular biology of the glia: Components of myelin—myelin basic protein—the implication of post-translational changes for demyelinating disease, in *Molecular Biology of Multiple Sclerosis* (Russell, W. C., Ed.) pp 37−54, John Wiley & Sons, New York.
11. Wood, D. D., and Moscarello, M. A. (1989) The isolation, characterization, and lipid-aggregating properties of a citrulline containing myelin basic protein, *J. Biol. Chem. 264*, 5121−5127.
12. Kim, J. K., Mastronardi, F. G., Wood, D. D., Lubman, D. M., Zand, R., and Moscarello, M. A. (2003) Multiple sclerosis: An important role for post-translational modifications of myelin basic protein in pathogenesis, *Mol. Cell. Proteomics 2*, 453−462.
13. Dunker, A. K., Brown, C. J., Lawson, J. D., Iakoucheva, L. M., and Obradovic, Z. (2002) Intrinsic disorder and protein function, *Biochemistry 41*, 6573−6582.
14. Libich, D. S., Hill, C. M. D., Bates, I. R., Hallett, F. R., Armstrong, S., Siemiarczuk, A., and Harauz, G. (2003) Interaction of the 18.5-kD isoform of myelin basic protein with $Ca^{2+}$-calmodulin: Effects of deimination assessed by intrinsic Trp fluorescence spectroscopy, dynamic light scattering, and circular dichroism, *Protein Sci. 12*, 1507−1521.
15. Boggs, J. M., Rangaraj, G., Hill, C. M., Bates, I. R., Heng, Y. M., and Harauz, G. (2005) Effect of arginine loss in myelin basic protein, as occurs in its deiminated charge isoform, on mediation of actin polymerization and actin binding to a lipid membrane in vitro, *Biochemistry 44*, 3524−3534.
16. Hill, C. M. D., and Harauz, G. (2005) Charge effects modulate actin assembly by classic myelin basic protein isoforms, *Biochem. Biophys. Res. Commun. 329*, 362−369.
17. Pirollet, F., Derancourt, J., Haiech, J., Job, D., and Margolis, R. L. (1992) $Ca^{2+}$-calmodulin regulated effectors of microtubule stability in bovine brain, *Biochemistry 31*, 8849−8855.
18. Wilson, R., and Brophy, P. J. (1989) Role for the oligodendrocyte cytoskeleton in myelination, *J. Neurosci. Res. 22*, 439−448.
19. Dyer, C. A., and Benjamins, J. A. (1989) Organization of oligodendroglial membrane sheets. I: Association of myelin basic protein and 2′,3′-cyclic nucleotide 3′-phosphohydrolase with cytoskeleton, *J. Neurosci. Res. 24*, 201−211.
20. Dyer, C. A., and Benjamins, J. A. (1989) Organization of oligodendroglial membrane sheets: II. Galactocerebroside:antibody interactions signal changes in cytoskeleton and myelin basic protein, *J. Neurosci. Res. 24*, 212−221.
21. Dyer, C. A., Philibotte, T. M., Billings-Gagliardi, S., and Wolf, M. K. (1995) Cytoskeleton in myelin-basic-protein-deficient shiverer oligodendrocytes, *Dev. Neurosci. 17*, 53−62.
22. Dyer, C. A., Philibotte, T. M., Wolf, M. K., and Billings-Gagliardi, S. (1994) Myelin basic protein mediates extracellular signals that regulate microtubule stability in oligodendrocyte membrane sheets, *J. Neurosci. Res. 39*, 97−107.
23. Dyer, C. A., Phillbotte, T., Wolf, M. K., and Billings-Gagliardi, S. (1997) Regulation of cytoskeleton by myelin components: Studies on shiverer oligodendrocytes carrying an Mbp transgene, *Dev. Neurosci. 19*, 395−409.
24. Boggs, J. M., Wang, H., Gao, W., Arvanitis, D. N., Gong, Y., and Min, W. (2004) A glycosynapse in myelin? *Glycoconjugate J. 21*, 97−110.

25. Modesti, N. M., and Barra, H. S. (1986) The interaction of myelin basic protein with tubulin and the inhibition of tubulin carboxypeptidase activity, *Biochem. Biophys. Res. Commun. 136*, 482−489.
26. Saoudi, Y., Paintrand, I., Multigner, L., and Job, D. (1995) Stabilization and bundling of subtilisin-treated microtubules induced by microtubule associated proteins, *J. Cell Sci. 108* (Part 1), 357−367.
27. Castoldi, M., and Popov, A. V. (2003) Purification of brain tubulin through two cycles of polymerization-depolymerization in a high-molarity buffer, *Protein Expression Purif. 32*, 83−88.
28. Ashford, A. J., Andersen, S. L. A., and Hyman, A. A. (1998) Preparation of tubulin from bovine brain, in *Cell Biology: A Laboratory Handbook* (Celis, J. E., Ed.) pp 205−212, Academic Press, New York.
29. Wood, D. D., Bilbao, J. M., O'Connors, P., and Moscarello, M. A. (1996) Acute multiple sclerosis (Marburg type) is associated with developmentally immature myelin basic protein, *Ann. Neurol. 40*, 18−24.
30. Bates, I. R., Matharu, P., Ishiyama, N., Rochon, D., Wood, D. D., Polverini, E., Moscarello, M. A., Viner, N. J., and Harauz, G. (2000) Characterization of a recombinant murine 18.5-kDa myelin basic protein, *Protein Expression Purif. 20*, 285−299.
31. Bates, I. R., Libich, D. S., Wood, D. D., Moscarello, M. A., and Harauz, G. (2002) An Arg/Lys→Gln mutant of recombinant murine myelin basic protein as a mimic of the deiminated form implicated in multiple sclerosis, *Protein Expression Purif. 25*, 330−341.
32. Hill, C. M. D., Haines, J. D., Antler, C. E., Bates, I. R., Libich, D. S., and Harauz, G. (2003) Terminal deletion mutants of myelin basic protein: New insights into self-association and phospholipid interactions, *Micron 34*, 25−37.
33. Lee, J. C., and Timasheff, S. N. (1977) *In vitro* reconstitution of calf brain microtubules: Effects of solution variables, *Biochemistry 16*, 1754−1764.
34. Kar, S., Fan, J., Smith, M. J., Goedert, M., and Amos, L. A. (2003) Repeat motifs of tau bind to the insides of microtubules in the absence of taxol, *EMBO J. 22*, 70−77.
35. Hoenger, A., Sablin, E. P., Vale, R. D., Fletterick, R. J., and Milligan, R. A. (1995) Three-dimensional structure of a tubulin-motor-protein complex, *Nature 376*, 271−274.
36. Herzog, W., and Weber, K. (1977) *In vitro* assembly of pure tubulin into microtubules in the absence of microtubule-associated proteins and glycerol, *Proc. Natl. Acad. Sci. U.S.A. 74*, 1860−1864.
37. Zhao, F. Q., and Craig, R. (2003) Capturing time-resolved changes in molecular structure by negative staining, *J. Struct. Biol. 141*, 43−52.
38. Tseng, H. C., and Graves, D. J. (1998) Natural methylamine osmolytes, trimethylamine-*N*-oxide and betaine, increase tau-induced polymerization of microtubules, *Biochem. Biophys. Res. Commun. 250*, 726−730.
39. Kim, H., Binder, L. I., and Rosenbaum, J. L. (1979) The periodic association of MAP2 with brain microtubules in vitro, *J. Cell Biol. 80*, 266−276.
40. Tseng, H. C., Lu, Q., Henderson, E., and Graves, D. J. (1999) Phosphorylated tau can promote tubulin assembly, *Proc. Natl. Acad. Sci. U.S.A. 96*, 9503−9508.
41. Zand, R., Li, M. X., Jin, X., and Lubman, D. (1998) Determination of the sites of posttranslational modifications in the charge isomers of bovine myelin basic protein by capillary electrophoresis-mass spectroscopy, *Biochemistry 37*, 2441−2449.
42. Pirollet, F., Margolis, R. L., and Job, D. (1992) $Ca^{2+}$-calmodulin regulated effectors of microtubule stability in neuronal tissues, *Biochim. Biophys. Acta 1160*, 113−119.
43. Boggs, J. M., Yip, P. M., Rangaraj, G., and Jo, E. (1997) Effect of posttranslational modifications to myelin basic protein on its ability to aggregate acidic lipid vesicles, *Biochemistry 36*, 5065−5071.
44. Bates, I. R., Boggs, J. M., Feix, J. B., and Harauz, G. (2003) Membrane-anchoring and charge effects in the interaction of myelin basic protein with lipid bilayers studied by site-directed spin labeling, *J. Biol. Chem. 278*, 29041−29047.
45. Ishiyama, N., Bates, I. R., Hill, C. M., Wood, D. D., Matharu, P., Viner, N. J., Moscarello, M. A., and Harauz, G. (2001) The effects of deimination of myelin basic protein on structures formed by its interaction with phosphoinositide-containing lipid monolayers, *J. Struct. Biol. 136*, 30−45.
46. Hill, C. M. D., Bates, I. R., White, G. F., Hallett, F. R., and Harauz, G. (2002) Effects of the osmolyte trimethylamine-*N*-oxide on conformation, self-association, and two-dimensional crystallization of myelin basic protein, *J. Struct. Biol. 139*, 13−26.
47. Polverini, E., Boggs, J. M., Bates, I. R., Harauz, G., and Cavatorta, P. (2004) Electron paramagnetic resonance spectroscopy and molecular modelling of the interaction of myelin basic protein (MBP) with calmodulin (CaM)-diversity and conformational adaptability of MBP CaM-targets, *J. Struct. Biol. 148*, 353−369.
48. Dobrowolski, Z., Osinska, H., Mossakowska, M., and Barylko, B. (1986) $Ca^{2+}$-calmodulin-dependent polymerization of actin by myelin basic protein, *Eur. J. Cell Biol. 42*, 17−26.
49. Devred, F., Barbier, P., Douillard, S., Monasterio, O., Andreu, J. M., and Peyrot, V. (2004) Tau induces ring and microtubule formation from $\alpha\beta$-tubulin dimers under nonassembly conditions, *Biochemistry 43*, 10520−10531.
50. Nogales, E., Wang, H. W., and Niederstrasser, H. (2003) Tubulin rings: Which way do they curve? *Curr. Opin. Struct. Biol. 13*, 256−261.
51. Wade, R. H., Pirollet, F., Margolis, R. L., Garel, J. R., and Job, D. (1989) Monotonic versus oscillating microtubule assembly: A cryo-electron microscope study, *Biol. Cell 65*, 37−44.
52. Gillespie, C. S., Wilson, R., Davidson, A., and Brophy, P. J. (1989) Characterization of a cytoskeletal matrix associated with myelin from rat brain, *Biochem. J. 260*, 689−696.
53. Karthigasan, J., Kosaras, B., Nguyen, J., and Kirschner, D. A. (1994) Protein and lipid composition of radial component-enriched CNS myelin, *J. Neurochem. 62*, 1203−1213.
54. Karthigasan, J., Garvey, J. S., Ramamurthy, G. V., and Kirschner, D. A. (1996) Immunolocalization of 17 and 21.5 kDa MBP isoforms in compact myelin and radial component, *J. Neurocytol. 25*, 1−7.
55. Karthigasan, J., Inouye, H., and Kirschner, D. A. (1995) Implications of the sequence similarities between tau and myelin basic protein, *Med. Hypotheses 45*, 235−240.
56. Jameson, L., Frey, T., Zeeberg, B., Dalldorf, F., and Caplow, M. (1980) Inhibition of microtubule assembly by phosphorylation of microtubule-associated proteins, *Biochemistry 19*, 2472−2479.
57. Murthy, A. S., and Flavin, M. (1983) Microtubule assembly using the microtubule-associated protein MAP-2 prepared in defined states of phosphorylation with protein kinase and phosphatase, *Eur. J. Biochem. 137*, 37−46.
58. Yamamoto, H., Fukunaga, K., Goto, S., Tanaka, E., and Miyamoto, E. (1985) $Ca^{2+}$-calmodulin-dependent regulation of microtubule formation via phosphorylation of microtubule-associated protein 2, tau factor, and tubulin, and comparison with the cyclic AMP-dependent phosphorylation, *J. Neurochem. 44*, 759−768.
59. Ainsztein, A. M., and Purich, D. L. (1994) Stimulation of tubulin polymerization by MAP-2. Control by protein kinase C-mediated phosphorylation at specific sites in the microtubule-binding region, *J. Biol. Chem. 269*, 28465−28471.
60. Csizmok, V., Bokor, M., Banki, P., Klement, E., Medzihradszky, K. F., Friedrich, P., Tompa, K., and Tompa, P. (2005) Primary contact sites in intrinsically unstructured proteins: The case of calpastatin and microtubule-associated protein 2, *Biochemistry 44*, 3955−3964.
61. Lee, Y. C., and Wolff, J. (1984) Calmodulin binds to both microtubule-associated protein 2 and tau proteins, *J. Biol. Chem. 259*, 1226−1230.
62. Evans, D. B., Rank, K. B., Bhattacharya, K., Thomsen, D. R., Gurney, M. E., and Sharma, S. K. (2000) Tau phosphorylation at serine 396 and serine 404 by human recombinant tau protein kinase II inhibits tau's ability to promote microtubule assembly, *J. Biol. Chem. 275*, 24977−24983.
63. Taniguchi, T., Kawamata, T., Mukai, H., Hasegawa, H., Isagawa, T., Yasuda, M., Hashimoto, T., Terashima, A., Nakai, M., Mori, H., Ono, Y., and Tanaka, C. (2001) Phosphorylation of tau is regulated by PKN, *J. Biol. Chem. 276*, 10025−10031.
64. Cho, J. H., and Johnson, G. V. (2004) Primed phosphorylation of tau at Thr231 by glycogen synthase kinase 3$\beta$ (GSK3$\beta$) plays a critical role in regulating tau's ability to bind and stabilize microtubules, *J. Neurochem. 88*, 349−358.
65. Feijoo, C., Campbell, D. G., Jakes, R., Goedert, M., and Cuenda, A. (2005) Evidence that phosphorylation of the microtubule-associated protein Tau by SAPK4/p38$\delta$ at Thr50 promotes microtubule assembly, *J. Cell Sci. 118*, 397−408.
66. Dyer, C. A. (2002) The structure and function of myelin: From inert membrane to perfusion pump, *Neurochem. Res. 27*, 1279−1292.

67. Vartanian, T., Szuchet, S., Dawson, G., and Campagnoni, A. T. (1986) Oligodendrocyte adhesion activates protein kinase C-mediated phosphorylation of myelin basic protein, *Science 234*, 1395−1398.
68. Mendieta, J., Fuertes, M. A., Kunjishapatham, R., Santa-Maria, I., Moreno, F. J., Alonso, C., Gago, F., Munoz, V., Avila, J., and Hernandez, F. (2005) Phosphorylation modulates the α-helical structure and polymerization of a peptide from the third tau microtubule-binding repeat, *Biochim. Biophys. Acta 1721*, 16−26.
69. Ramwani, J. J., Epand, R. M., and Moscarello, M. A. (1989) Secondary structure of charge isomers of myelin basic protein before and after phosphorylation, *Biochemistry 28*, 6538−6543.
70. Deibler, G. E., Stone, A. L., and Kies, M. W. (1990) Role of phosphorylation in conformational adaptability of bovine myelin basic protein, *Proteins 7*, 32−40.
71. Andrew, C. D., Warwicker, J., Jones, G. R., and Doig, A. J. (2002) Effect of phosphorylation on α-helix stability as a function of position, *Biochemistry 41*, 1897−1905.
72. Bates, I. R., and Harauz, G. (2003) Molecular dynamics exposes α-helices in myelin basic protein, *J. Mol. Model. 9*, 290−297.
73. Fuxreiter, M., Simon, I., Friedrich, P., and Tompa, P. (2004) Preformed structural elements feature in partner recognition by intrinsically unstructured proteins, *J. Mol. Biol. 338*, 1015−1026.
74. Dyson, H. J., and Wright, P. E. (2005) Intrinsically unstructured proteins and their functions, *Nat. Rev. Mol. Cell Biol. 6*, 197−208.
75. Smith, M. J., Crowther, R. A., and Goedert, M. (2000) The natural osmolyte trimethylamine-*N*-oxide (TMAO) restores the ability of mutant tau to promote microtubule assembly, *FEBS Lett. 484*, 265−270.
76. Ozer, R. S., and Halpain, S. (2000) Phosphorylation-dependent localization of microtubule-associated protein MAP2c to the actin cytoskeleton, *Mol. Biol. Cell 11*, 3573−3587.
77. Dyer, C. A., and Benjamins, J. A. (1990) Glycolipids and transmembrane signaling: Antibodies to galactocerebroside cause an influx of calcium in oligodendrocytes, *J. Cell Biol. 111*, 625−633.
78. DeBruin, L. S., Haines, J. D., Wellhauser, L. A., Radeva, G., Schonmann, V., Bienzle, D., and Harauz, G. (2005) Developmental partitioning of myelin basic protein into membrane microdomains, *J. Neurosci. Res. 80*, 211−225.
79. Dyer, C. A., and Matthieu, J. M. (1994) Antibodies to myelin/oligodendrocyte-specific protein and myelin/oligodendrocyte glycoprotein signal distinct changes in the organization of cultured oligodendroglial membrane sheets, *J. Neurochem. 62*, 777−787.
80. Dyer, C. A. (1997) Myelin proteins as mediators of signal transduction, in *Cell biology and pathology of myelin: Evolving biological concepts and therapeutic approaches* (Juurlink, B. H. J., Devon, R. M., Doucette, J. R., Nazarali, A. J., Schreyer, D. J., and Verge, V. M. K., Eds.) pp 69−74, Plenum Press, New York.
81. Lintner, R. N., and Dyer, C. A. (2000) Redistribution of cholesterol in oligodendrocyte membrane sheets after activation of distinct signal transduction pathways, *J. Neurosci. Res. 60*, 437−449.
82. Boggs, J. M., and Wang, H. (2004) Co-clustering of galactosylceramide and membrane proteins in oligodendrocyte membranes on interaction with polyvalent carbohydrate and prevention by an intact cytoskeleton, *J. Neurosci. Res. 76*, 342−355.
83. Boggs, J. M., and Rangaraj, G. (2000) Interaction of lipid-bound myelin basic protein with actin filaments and calmodulin, *Biochemistry 39*, 7799−7806.
84. Yamauchi, P. S., and Purich, D. L. (1993) Microtubule-associated protein interactions with actin filaments: Evidence for differential behavior of neuronal MAP-2 and tau in the presence of phosphatidyl-inositol, *Biochem. Biophys. Res. Commun. 190*, 710−715.

BI050646+